MICROSTRUCTURAL EVALUATION DURING MECHANICAL ALLOYING AND AIR CONSOLIDATION OF Fe_3Al + (Li, Ni AND C) INTERMETALLIC.

J. Chihuaque[a], C. Patiño-Carachure[a], J.O. Téllez-Vázquez[a], A.Torres-Islas[b] and G. Rosas*[a]

[a]Instituto de Investigaciones Metalúrgicas, UMSNH P. O. Box 52-B, 58000 Morelia, Mich., México
[b]Centro de Investigación en Ingeniería y Ciencias Aplicadas, UAEM, Cuernavaca, Mor. 62210, México

*Corresponding author, E-mail: grtrejo@umich.mx. (52443) 3223500, ext. 4032.

Recibido: Julio 2010. Aprobado: Septiembre 2010.
Publicado: Noviembre 2010.

ABSTRACT
In this investigation, Fe_3Al intermetallic nanocrystalline powders with C, Ni y Li additions were produced by mechanical alloying. These powders were consolidated under uniaxial compressive pressure and a sintering process in air. Analytical techniques such as; scanning electron microscopy, transmission electron microscopy, differential scanning calorimetry have been used for the morphological and chemical characterization of the alloyed powders. Additions of C, Ni and Li to Fe_3Al have been explored as reinforced elements to improve the mechanical properties. The results indicate that the intermetallic alloy is formed from Fe and Al elemental powders after 7 h of milling time. The elements are dissolved in the Fe_3Al structure. Density of the compact varied according to the different added elements. The microstructures and density measurements showed relatively good densification near to 90%. However, the best densification values were obtained with Ni and Li additions. The average crystal size of the consolidated specimen was found to be up to 300 nanometers indicating crystal growth occurred during consolidation. The increase in hardness values with element additions may be attributed to the formation of higher densities of lattice defects during mechanical alloying and the presence of Al_2O_3 compound.

Keywords: Iron aluminides; uniaxial compaction; Fe_3Al intermetallic; Hardness; Mechanical Alloying.

EVALUACIÓN MICROESTRUCTURAL DURANTE EL ALEADO MECÁNICO Y LA CONSOLIDACIÓN EN AIRE DEL INTERMETÁLICO Fe_3Al+(Li, Ni Y C).

RESUMEN
En esta investigación se obtuvieron, mediante el proceso de aleado mecánico, polvos nanocristalinos del intermetálico Fe_3Al con adiciones de C, Ni y Li. Estos polvos fueron consolidados bajo presión uniaxial y sinterizado en aire. La caracterización morfológica y química de la aleación se realizó utilizando técnicas analíticas tales como; microscopía electrónica de barrido (MEB), microscopía electrónica de transmisión, y calorimetría de barrido diferencial. La adición de C, Ni y Li a la aleación intermetálica se realizó con la finalidad de evaluar el comportamiento de los elementos para mejorar las propiedades mecánicas. Los resultados de difracción de rayos X indican que después de 7 horas y partiendo de polvos elementales de Fe y Al, la aleación intermetálica se efectúa, los elementos menores se disuelven en la estructura intermetálica de Fe_3Al. Las microestructuras obtenidas por MEB y las mediciones de densidad, mostraron una relativa buena densificación de los compactos cercana al 90%, sin embargo, los mejores valores se obtuvieron con las adiciones de Ni y Li. El promedio del tamaño de los cristales en las muestras sinterizadas fue superior a los 300 nanómetros, indicando que el crecimiento cristalino ocurre durante la sinterización. El incremento en los valores de dureza con la adición de los diferentes elementos, puede ser atribuido a la formación de una alta densidad de defectos de red durante el proceso de aleado mecánico y la presencia de partículas del compuesto Al_2O_3.

Palabras claves: Aluminuros de hierro, Compactación uniaxial, Intermetálico Fe_3Al, Dureza, Aleado Mecánico.

INTRODUCTION

Iron aluminides based on Fe_3Al offer advantages for structural uses at elevated temperatures because of their excellent oxidation resistance, good mechanical properties, relatively low cost and material density [1-4]. However, the applications of these intermetallics have been limited due to their brittle nature at room temperature an environmental hydrogen embrittlement [2]. Considerable studies have been conducted to improve their mechanical properties through control of

microalloying [3,4], alloy composition [5] and processing techniques [6]. For example, mechanical alloying technique has been used in the past to obtain intermetallic compounds with nanometric size ranges [7]. In addition, mechanical alloying eliminates the chemical segregation, large grain boundaries and increases the solid solubility. These microstructural defects affect their mechanical properties of intermetallic alloys [8,9]. Another attribute of mechanically alloying is the disordering of intermetallic compounds [9-12]. Past investigations have shown that Fe_3Al microalloying with Li and Ni passivity the hydrogen embrittlement in alloys produced by rapid solidification [13]. In addition, Li additions improve the mechanical properties of Fe_3Al in samples produced by conventional casting [14]. Thus, in this investigation, different Fe_3Al intermetallic alloys with C, Li and Ni additions were obtained used mechanical alloying. The mechanical alloyed powders were consolidated using a uniaxial hydraulic press, and subsequently the specimens were annealed in air.

The microstructural features of these alloys were studied by X-ray diffraction, scanning electron microscopy, transmission electron microscopy and DSC-TGA thermal experiments. Finally, hardness RC (HRC) measurements were carrying out to understand the mechanical properties of these alloys.

MATERIALS AND METHODS

The mechanical alloying experiments on the Fe_3Al-X (X = C, Ni, Li) powder mixtures were performed in a vibratory ball-mill (SPEX 8000) using hardened steel vials and balls. In these experiments, high purity elemental powders (99.9%) were weighed to give the nominal compositions of $Fe_{74}Al_{25}Li_1$, $Fe_{74}Al_{25}Ni_1$, $Fe_{74}Al_{25}C_1$ mixed in a glove box under a purified argon atmosphere. The samples were milled for 1, 2, 3, 4, 5, 6 and 7 h, and methanol was added as a process control agent (0.075 ml by gram) to prevent excessive welding. The mechanically-milled powders were compacted using uniaxial hydraulic press under an applied pressure of 1170MPa to obtain disc samples with a depth of ~5 mm. The compacted material was annealed in air at 1100 ^oC for 1 h. Density measurements based on the Archimedes approach were carried out on the green and the annealed specimens. HRC values were obtained from the sintered specimens using a WILSON Mod. 5JP indenter with a load of 150 Kg. The hardness values reported are averaged from six indentation results. Microstructural and chemical characteristics of the powders were observed using X-ray diffraction (Siemens D5000), and scanning and transmission electron microscopy (Jeol 6400, FEG Philips Tecnai F20).

RESULTS AND DISCUSSION

Figure 1 shows X-ray diffraction patterns for a series of samples with nominal compositions of $Fe_{75}Al_{25}$. The initial XRD pattern (0 h) displays the pure elemental Fe and Al patterns. As the milling time was increased from 1 to 7 h, the peaks intensities diminished and become wider suggesting nanometric size crystals and lattice micro-strains. The XRD patterns only shows one peak at 44.1º which could be belong to the Fe_3Al DO_3 structure formation, but this peak can also be indexed with the (110) reflection of Fe bcc. It can be seen that the diffraction peaks tends to move toward smaller angles. This could be a sign of the aluminum-iron solubility in the mechanically milled samples.

In order to have more insight into the aluminum-iron solubility after mechanical milling, a DSC analysis was carried out. Figure 2 illustrates a DSC graph for the $Fe_{75}Al_{25}$ alloy milled for 7 h. An endothermic peak approximately at 1300 ^oC related to the intermetallic melting point can be clearly observed. This result suggest the mechanical alloying of the Al and Fe elemental powders and confirms that, the XRD diffraction peak in figure 1, correspond to the iron-aluminum solubility to form the Fe_3Al intermetallic.

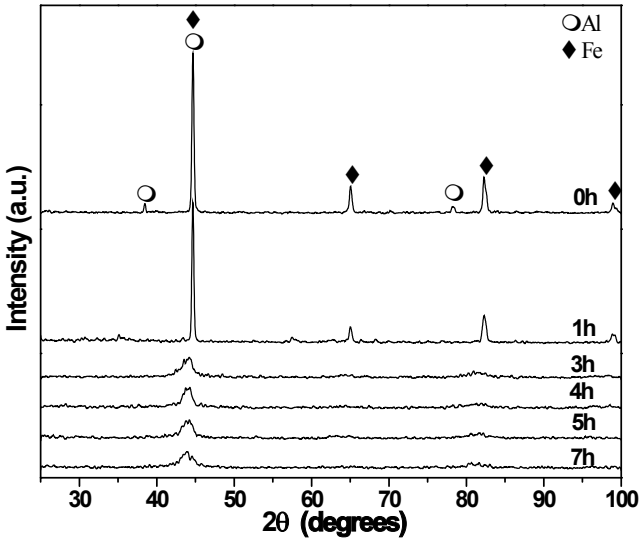

Fig. 1. XRD patterns of as-cast and ball-milled samples.

The milled powders were also examined by transmission electron microscopy. Figure 3a, shows an electron diffraction pattern (EDP) of concentric rings obtained as a result of the smaller crystal size, evidencing the nanocrystalline nature of the Fe_3Al alloy. Measurements on the polycrystalline diffraction pattern correspond to the sequence of planes which belong to Miller indices (220), (400), (420) and (440). This sequence is part of the Fe_3Al intermetallic phase which has a DO_3 structure type. Figure 3b shows the dark-field image of the same specimen where bright- spots contrasts are nanocrystals having a size of less than 20 nm.

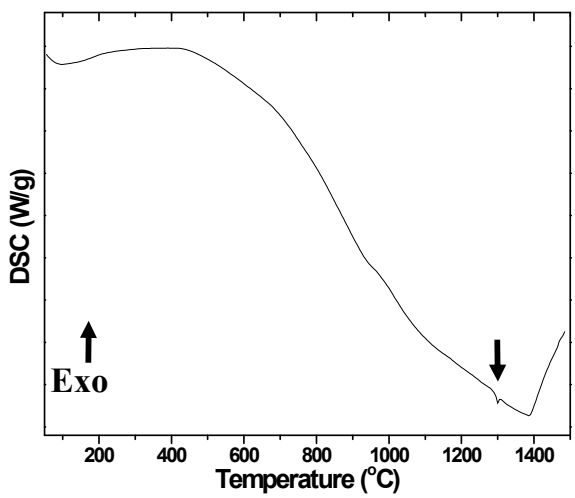

Fig. 2. DSC-graph of Fe_3Al powders ball-milled sample for 7 h.

On the other hand, figure 3c shows a bright-field TEM image of Fe_3Al+Ni alloy composition after 7 h of ball-milling. This image suggests that the nanocrystals are embedded in an amorphous matrix. Moiré fringes are frequently observed with spacing between 10 to 20 nm. Moiré contrast is caused by nanograins that lie on top of each other. In addition, figure 3d illustrates a HRTEM image of small crystal with lattice fringes of about 0.205 nm which approximately correspond to the (202) planes of the intermetallic structure. This image shows variations in the intensities of the lattice fringes which may be due to the presence of antiphase boundaries typical of ordered materials.

SEM technique analysis was conducted to evaluate the shape and size of the Fe_3Al particles. The initial morphology of the Fe elemental powders are shown in Figure 4a. Fe particles show spherical-like morphology but, the Al powders present random shape and size morphology (not illustrated). Figures 4b and c show flat particles morphology obtained by a heavy mechanical deformation after 1 and 2 h of milling time respectively. High deformation of the particles leads to the welding of the flat particles to form sandwich particles [15] with an average diameter of nearly 10 μm. During the subsequent stages of milling the hardened of the agglomerated particles is increased due to the increment of cold working that induces several crystalline defects [16]. These agglomerated hardened particles tend to the fragmentation process to form finer powders with wide particle size distribution. A balance between fracturing and cold welding is obtained after 4 h (Figures 4d-e) of milling; the particle size and the particle size distribution tend to an average diameter of around 8 μm. Figure 4f show a SEM image of the final alloyed powders, at this stage of milling (7 h) an interdiffusion reaction takes place inside the clean surfaces of the intimate layers of the particles to form the Fe_3Al intermetallic alloy (16).

Figures 5a-d illustrates SEM images and its corresponding SAD patterns obtained after mechanical process of Fe_3Al intermetallic and for the different alloying elements. These results correspond to experiments using balls of 1/2" diameter and a ball-to-powder weight ratio of 11:1.

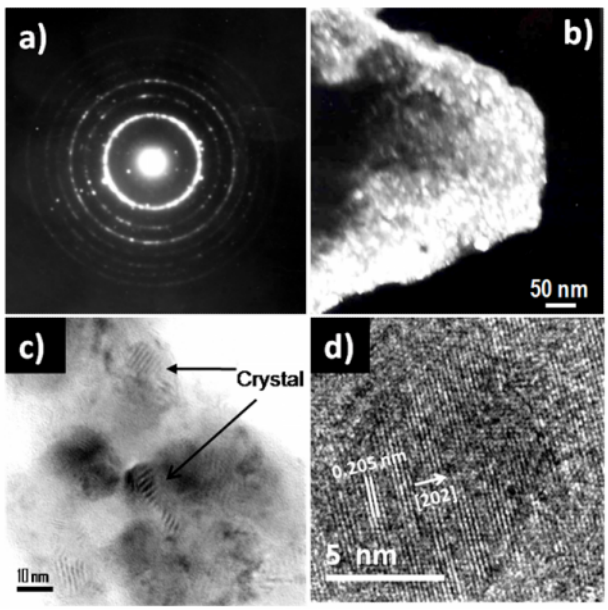

Fig. 3. TEM illustrations of ball-milled samples; a) SAD polycrystalline pattern of Fe_3Al intermetallic alloy milled for 7 h and b) their corresponding dark-field image, c) Bright-field image of the Fe_3Al+Ni ball-milled powders for 7 h. and finally d) HRTEM image of intermetallic milled powders for 7 h.

As can be seen the milled intermetallic powders with additions of lithium showed the smaller particle size and homogeneous particle size distribution (Figure 5). The SAD patterns show the polycrystalline nature of the powders as consequence of small crystal size. This is similar to the results obtained from Fe_3Al without additions (Fig. 5a). A more refined structure is observed in the samples with Ni and Li additions (figure 5c and 5b). However, extra spots are presents mainly in the Fe_3Al (figure 5a) and Fe_3Al + C (figure 5b) alloys which indicate some large grains.

The mechanical alloyed powders were consolidated at room temperature using a uniaxial-hydraulic press. Figure 6a-d show SEM images of the cross-sectional microstructure from the different additions to Fe_3Al alloys. The microstructure of the consolidated samples revealed agglomerates consisting of grains (3-4 μm) intermingled with larger grains (greater than 10 μm).

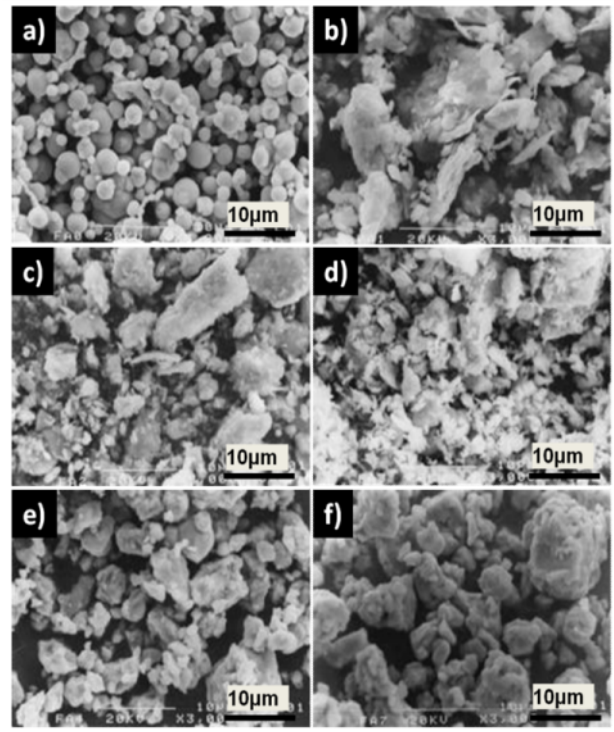

Fig. 4. SEM images of the Fe_3Al powders samples for a) 0 h, b) 1 h, c) 2 h, d) 4 h, e) 5 h and f) 7 h of ball-milling.

These pictures suggest that the best sintering conditions were achieved for samples with Ni (fig.6c) and Li (fig. 6d) additions, followed by C (fig. 6b), and finally for the Fe_3Al without additions (fig. 6a). The microstructure of the Li additions shows the smaller agglomeration size. This is probably influenced by the smaller particle size obtained as a result of the mechanical milling before the sintering process.

The densification and hardness values of the Fe_3Al intermetallic alloy obtained without and also with different elements additions (Li, C, Ni) before and after sintering process are illustrated in Fig. 7. These results correspond to the annealed samples at 1100 ºC for 1h and

consolidated at 1170 MPa. Sintered densities near to 90% were obtained. Highest densification values correspond to the Ni and Li additions, while lowest densification values were obtained in the case of carbon additions. These densification values are relatively lower in comparison with those obtained with other compaction techniques [17]. However, the hardness values in the case of Li addition are lower to those obtained with conventional solidification techniques [14]. This result can improve the mechanical properties of intermetallic alloy. In the Ni additions case the hardness values are increased in comparison to those obtained from conventional solidification techniques [14]. This result can improve the strength of intermetallic alloy.

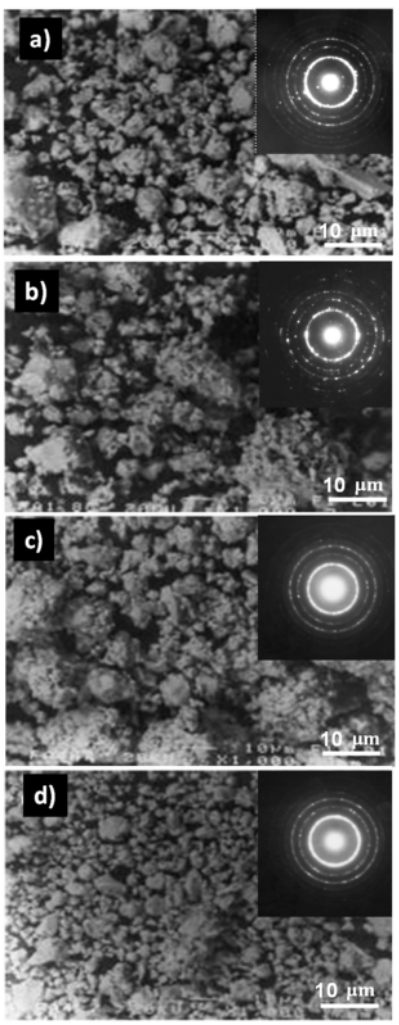

Fig. 5. SEM images and its corresponding SAD patterns from the different Fe_3Al intermetallic powders, a) Fe_3Al, b) Fe_3Al + C , c) Fe_3Al + Ni and d) Fe_3Al + Li.

The XRD patterns from the sintered specimens with the addition of the different elements were also obtained. The diffraction patterns are illustrated in Fig. 8, where the presences of the Fe_3Al and Al_2O_3 phases were clearly identified.

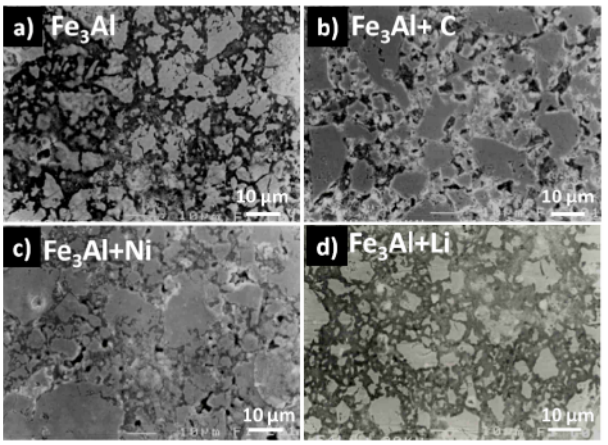

Fig. 6. SEM micrographs of the compacts; a) without and b), c), d) with different alloying elements.

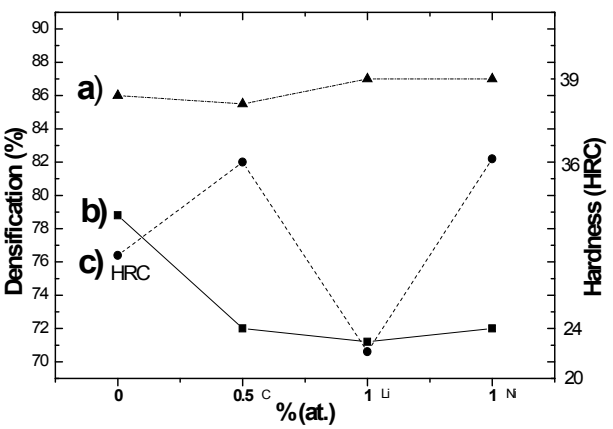

Fig. 7. Densification values obtained as a function of the alloyed minor elements; a) after and b) before sintering process, c) hardness values of the compacts.

The average grain size of these consolidated samples is about 300 nm, therefore, the sintered sample loss the nanocrystalline character. However, the consolidation samples do not lead to any structural changes in the sintered Fe_3Al material.

CONCLUSIONS

Intermetallic alloys of Fe_3Al with C, Ni and Li addition were fabricated using high-energy ball milling and consolidated by a uniaxial hydraulic press. The addition of different elements to the Fe_3Al intermetallic compound has a slightly influence on the size, distribution and compaction of the powder particles. Sintered densities near to 90% were obtained. The highest densification values were obtained in the case of Ni and Li additions. Furthermore, in the case of lithium additions lowest hardness values were obtained. The sintered specimens, however, have Al_2O_3 phase, which could contribute to hardness increase and consequently increase of intermetallic strength.

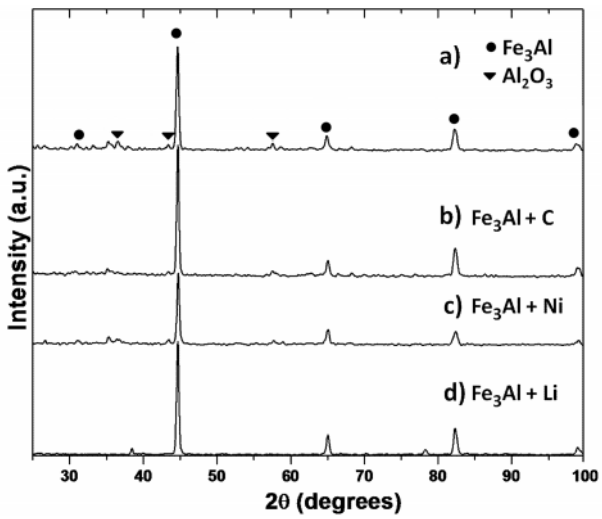

Figure 8. X-ray diffraction patterns obtained from the sintered alloy a) Fe_3Al without any element addition and b), c) and d), with C, Ni and Li element additions, respectively.

ACKNOWLEDGMENTS

A.Torres-Islas acknowledge CONACYT support through their "Convocatoria 2009 de Estancias posdoctorales y sabáticas vinculadas al fortalecimiento de la calidad del posgrado nacional modalidad A en IIM-UMSNH". G. Rosas would like to thank the financial support received from the National Council for Science and Technology of Mexico (CONACYT) under the grant 48716-25535.

REFERENCES

[1] Anita Olszowka-Myalska, Wojciech Maziarz (2006) "Microstructural analysis of iron aluminide formed by self-propagating high temperature synthesis mechanism in aluminum matrix composite" J. *Microscopy* 224(1):1-3.

[2] Gilbert Hénaff, Anne Tonneau (2001) "Environment-sensitive fracture of iron aluminides under monotonic tensile loading" *Metall. Mater. Trans. A* 32A:557-567.

[3] Garima Sharma, R.V. Ramanujan, T.R.G. Kutty, N. Prabhu (2005) "Indentation creep studies of iron aluminide intermetallic alloy" *Intermetallics* 13(1):47-53.

[4] J. Ritherdon, A.R. Jones and I.G. Wright (2001) "The recovery and recrystallization of a mechanically alloyed ODS-Fe_3Al alloy" *Mater.Sci. Forum* 360-362:217-222.

[5] W. Deng, R.S. Brusa, G.P. Karwasz, A. Zecca (2001) "Defect Studies in Fe_3Al Alloys doped with Cr, Mo and Si" *Materials Science Forum 363-365*:195-197.

[6] Hao Chuncheng, Cui Zuolin, Yin Yansheng, Zhang Zhikum (2002) "Preparation and mechanical properties of Fe_3Al nanostructured intermetallics" *J. Nanopart. Res.* 4:107-110.

[7] G. Gonzalez, L.D'Angelo, J. Ochoa, L.D'Onofrio (2001) "Study of the synthesis and sintering of nanophase $Fe_{73}Al_{27}$ obtained by mechanical alloying" *Materials Science Forum* 360-362: 349-354.

[8] M. Salazar, A. Albiter, G. Rosas, R. Perez (2003) "Structural and mechanical properties of the AlFe intermetallic alloy with Li, Ce and Ni additions" *Mater.Sci. Eng. A* 351:154-159.

[9] M.H. Enayati, M. Salehi (2005) "Formation mechanism of Fe_3Al and FeAl intermetallic

compounds during mechanical alloying" *J.Mater.Sci.* 40(15):3933-3938.

[10] Jian Wang, Jiandong Xing, Zhibin Qiu, Xiaohui Zhi, Li Cao (2009) "Effect of fabrication methods on microstructure and mechanical properties of Fe3Al-based alloys" *Journal of Alloys and Compounds* 488:117–122.

[11] Jian Wang, Jiandong Xing, Li Cao, Wei Su, Yimin Gao (2010) "Dry sliding wear behavior of Fe3Al alloys prepared by mechanical alloying and plasma activated sintering" *Wear* 268:473–480.

[12] M. Khodaei, M.H. Enayati, F. Karimzadeh (2009) "The structure and mechanical properties of Fe3Al–30 vol.% Al2O3 nanocomposite" *Journal of Alloys and Compounds* 488:134–137.

[13] M. Salazar, R. Perez, G. Rosas (2005) "Environmental embrittlement characteristics of the AlFe and AlCuFe intermetallic systems" *J. New Mater. Electrochem. Syst.* 8:97-100.

[14] G. Rosas, R. Esparza, A. Bedolla-Jacuinde, R. Perez (2009) "Room temperature mechanical properties of Fe_3Al intermetallic alloys with Li and Ni additions" *J. Mater.Eng. Perform.* 18(1):57-61.

[15] P.S. Gilman and J.S. Benjamin (1983) **"**Mechanical-alloying" *Annu. Rev. Mater. Sci.* 13:279-300.

[16] C. Suryanarayana, E. Ivanov, V.V. Boldyrev (2001) "The science and technology of mechanical alloying" *Mater. Sci. Eng. A* 304-306:151–158.

[17] Frederic Bernard, Frederic Charlot, Eric Gaffet, Zuhair A. Munir (2001) "One step Synthesis and consolidation of nanophase iron aluminide" *J. Am. Ceram. Soc.* 84(5):910-914.